



## Analytical Study of Free Vibration Characteristics For Sandwich Cylindrical Shell With Single Phase Metal Core

Ahmed Mouthanna<sup>a\*</sup>, Sadeq H. Bakhy<sup>a</sup>, Muhannad Al-Waily<sup>b</sup>

<sup>a</sup> Mechanical Engineering Dept., University of Technology-Iraq, Alsina'a street, 10066 Baghdad, Iraq.

<sup>b</sup> Mechanical Engineering Dept., Faculty of Engineering, University of Kufa, Iraq.

\*Corresponding author Email: [me.20.26@grad.uotechnology.edu.iq](mailto:me.20.26@grad.uotechnology.edu.iq)

### HIGHLIGHTS

- A novel sandwich cylindrical shell made of single-phase FG porous core.
- Used analytical approach based on the classical shell theory and fourth-order Runge-Kutta technique.
- FGMs are important components of different engineering applications.
- Porosity increases raise natural frequencies, while gradient index increases decrease them in FGM cylindrical shells.
- Polyethylene has a high nonlinear vibration response due to its low stiffness.

### ARTICLE INFO

**Handling editor:** Sattar Aljabair

**Keywords:**

Nonlinear Free vibration  
Analytical Technique  
Functionally graded materials  
Porous metal  
Sandwich Shell

### ABSTRACT

This paper presents an analytical investigation of the nonlinear vibration characteristics of a single-phase functionally graded cylindrical shell panel with various porous metal cores. Porous constructions with varying degrees of porosity throughout their volume are known as functionally graded materials (FGMs). These materials have a wide range of applications across several industries, including shipbuilding, automotive, biomedical, marine, and aerospace. The sandwich cylindrical panel has a porous metal core, while the top and bottom faces are composed of homogeneous materials. The model is improved using a power-law function. The governing equations of motion are discretized according to the classical thin shell theory with von Karman nonlinear strain-displacement relations by applying Galerkin's method to a collection of ordinary nonlinear equations. The nonlinear equations are determined using the fourth-order Runge-Kutta method, which is implemented in MATLAB software. The influences of core materials, porosity distribution, FG core thickness, face sheet layers, and changing gradient index on the natural frequency and dynamic response of the FG cylindrical shell are discussed. The existing literature is used to compare the current findings, and a favorable level of consistency is observed. The results obtained indicate that the porosity coefficients have a notable impact on the vibration behavior and overall reliability of functionally graded structures. The results demonstrate that when the porous parameter is increased, the natural frequencies of the FG sandwich cylindrical also increase. Nevertheless, this paper also presents several new and valuable results that may be of great reference to the readers.

## 1. Introduction

FGMs are novel, complex composite materials that are microscopically inhomogeneous and have mechanical properties that change constantly and smoothly from one surface to another [1]. Compared to conventional composites, these materials provide several benefits, especially when employed at high temperatures. One of the most significant structures, curved panels are commonly applied in civil and mechanical engineering. FGM-based cylindrical panels are commonly employed in biomedical applications, electronic devices, automobiles, aerospace, and aircraft [2]. Polyethylene sandwich cylindrical shell panels are extensively used in different engineering applications, including aerospace, automobile, and naval industries, because of their excellent mechanical properties and lightweight nature [3].

Numerous study articles have been published on the advanced FG material, which has attracted the attention of scientists worldwide. Srivastava et al. [4] presented an approach to create and manufacture FGM utilizing the fused deposition modeling technique. Luat et al. [5] explored the bending, free vibration, and buckling analysis of a new bifunctionally graded sandwich nanobeam, employing a refined, non-local, simple shear deformation theory. Do et al. [6] developed a refined plate theory to analyse the static bending behaviour of plates made of functionally graded materials. Deepak and Shetty [7] investigated the static and free vibration behavior of FGM rectangular plates by employing ANSYS. Gantayat et al. [8] investigated the dynamic characteristics of an axial FGM using the finite element method. Thom et al. [9,10] discussed the results of a study that used the

finite element method and phase field theory to examine the vibration response and buckling behaviour of a cracked FGM plate. Karakoti et al. [11] focused on the bending analysis of sandwich shell panels that have an exponentially graded core with top and bottom face sheets made of pure ceramic and pure metal using a finite element formulation and first-order shear deformation theory. Hadi and Ameen [12] used the finite element technique and higher-order shear deformation theory to investigate the nonlinear free vibration behaviour of cylindrical shells, Jweeg et al. [13] analysed the dynamic characteristics of a hybrid conical shell construction using theory and experimental methods. Medjmadj et al. [14] studied the experimental manufacturing, thermal, mechanical and physical properties of sandwich structures made of similar polymer skins and cork or plaster with functionally graded cores. Dat et al. [15] used the finite element method to investigate the free vibration of sandwich plates with stiffeners made of functionally graded materials. Cong and Duc [16] dissected the nonlinear thermal vibration behavior of eccentrically stiffened auxetic honeycomb sandwich cylindrical shells under temperature-dependent characteristics. Anh et al. [17] provided an analytical solution that demonstrates how the vibration of sandwich double-curved shallow shells that is affected by geometrical and material parameters, as well as stiffeners, is affected by blast loading, temperature and visco-Pasternak medium. Zghal et al. [18] used improved finite shell elements to study the free vibration of FG panels and plates in a thermal environment. Ahmadi et al. [19] presented the dynamic features of imperfect FG-stiffened shallow shells resting on elastic foundations utilizing the multiple-scales approach. Njim et al. [20,26] presented a numerical, analytical, and experimental examination of the free vibration and buckling properties and their optimisations in a porous FGM sandwich plate with different boundary conditions. Ebrahimi et al. [27] analysed the vibration characteristics of metal porous foam plates that rest on the viscoelastic. Kumar et al. [28] researched the impact of variable thickness on the vibration characteristics of porous FGM plates with the Pasternak foundation. Hadji and Avcar [29] investigated the free vibration of sandwich porous FG plates under different boundary conditions using higher-order shear deformation plate theory. Oveissi et al. [30,31] explored the impact of small-scale nanoflow and nanostructure on the vibrational response of fluid flowing through single-walled carbon nanotubes. Mohammadi et al. [32] investigated the free vibration behaviour of nanocomposite panels designed with a free-form curve that slid along a straight line. Mohammadi [33] studied the thermal buckling of laminated panels made of functionally graded trapezoidal corrugated graphene platelet reinforced composite (FG-GPLRC) using higher-order shear deformation theory. Wang et al. [34] investigated the nonlinear dynamics of primary resonance in truncated conical microshells (TSMs) composed of magnetostrictive face sheets with functionally graded material (FGM), which are subject to an external magnetic field and mechanical harmonic soft excitation. Dat et al. [35] focused on the impact of porosity, CNTs, and thermal and mechanical loading on the non-linear dynamic properties of the sandwiched FG carbon nanotube-reinforced composite plate. Mouthanna et al. [36,37] studied the nonlinear vibration properties of the porous ES-FGM cylinder panels. Mirjavadi et al. [38] explored the nonlinear free vibrations of elastically surrounding and circumferentially stiffening porous FG annular spherical shell segments. Karakoti et al. [39] analysed the non-linear transient response of porous sandwich Sigmoid-FGM and Power-FGM shell panels and plates subjected to a thermal environment and blast loading. Sobhani et al. [40] analysed the frequencies of the free-damped vibration characteristics of tangential waves in hemispherical cylinder shells merged with FG sandwich that were subjected to elastic springs. Mohammadi et al. [41-43] offered the free vibration and buckling analysis of trapezoidally corrugated functionally graded graphene-reinforced composite laminated plates and panels using higher-order shear deformation theory with isogeometric analysis.

Previous studies on vibration problems and the investigation of buckling of porous FGMs have focused mainly on two-phase materials, such as ceramic metals, for the core. There has been limited research on the use of single-phase metal cores throughout the entire thickness of the shell to create FG properties. The novelty of this paper lies in using a single-phase metal core for the FG sandwich-shell structure and examining its vibration behaviour. The non-linear dynamic behaviour of porous cylindrical FGM shell panels is described in this paper. The governing equation is derived from the classical shell theory with geometrical nonlinearity. The non-linear transients curve of cylindrical panels is estimated on the basis of the displacement response utilising the fourth-order Runge-Kutta methods.

## 2. FGM Cylindrical Panels

Consider a sandwich FGM cylindrical panel as displayed in Figure 1a. The thickness, length of the panel, axial length, and curvature radii are  $h$ ,  $b$ ,  $a$ , and  $R$ , respectively. The sandwich cylindrical panel consists of three layers, which are two homogeneous face sheets and a functionally graded (FG) porous core. The dimensions of the sandwich panel are shown in Figure 1b, where  $h_l$  and  $h_U$  have equal thicknesses and are made of the same homogeneous materials. The values  $z_0$ ,  $z_1$ ,  $z_2$ , and  $z_3$  represent the thicknesses at different points of the panel. The following power law distribution is supposed to apply to the volume fractions of components for the FGM shell as it varies in thickness direction [44,45] :

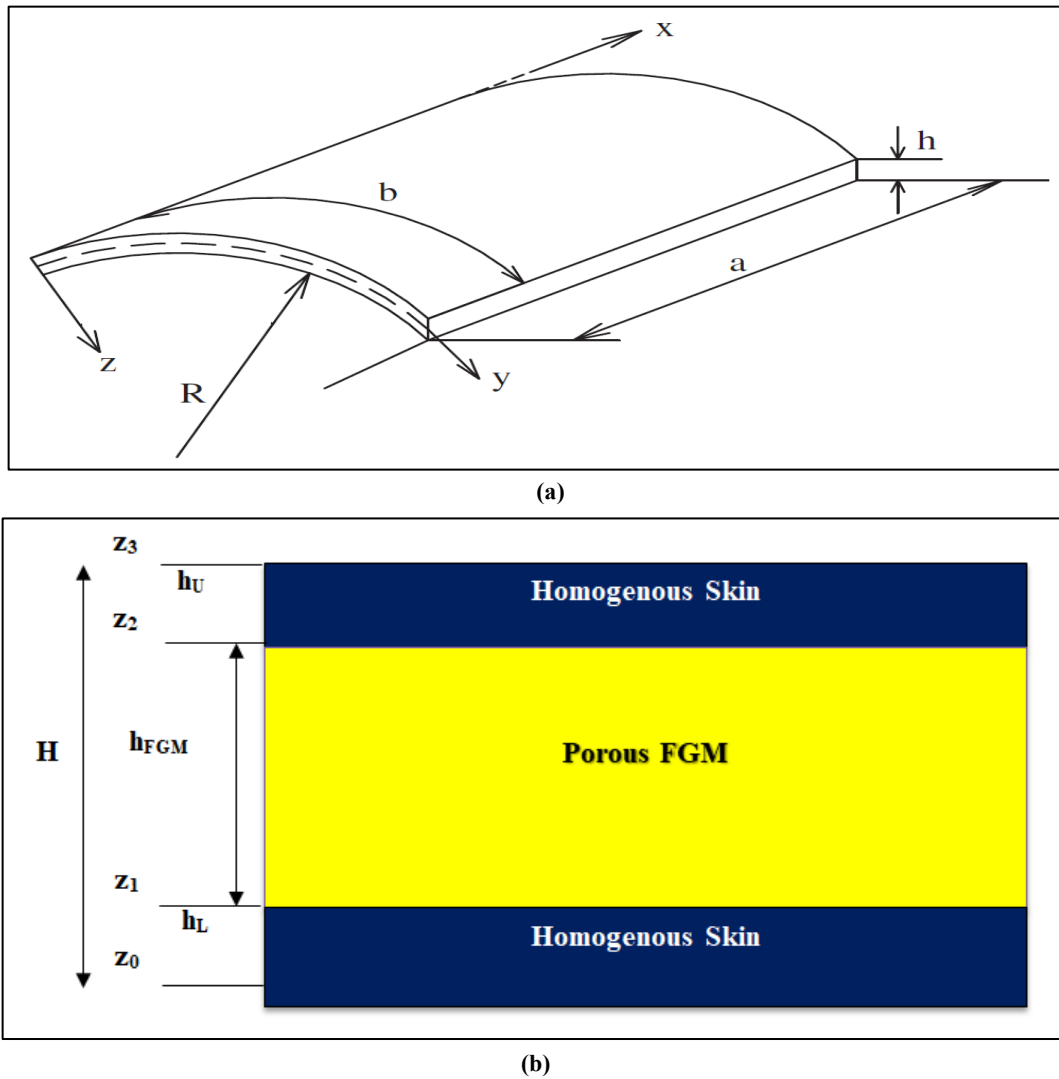


Figure 1: The geometry of the cylindrical porous FGM sandwich shell

$$V_m(z) = \left(\frac{2z+h}{2h}\right)^k, V_c(z) = 1 - V_m(z), \tag{1}$$

where  $k$  is the material gradient. According to the power law distribution, it is assumed in this study that FGMs are a composite of single-phase metal. The formula for the material coefficient  $P(z)$  is as follows:

$$P(z) = P_m - \beta \cdot P_m \left(\frac{z}{h} + \frac{1}{2}\right)^k, \tag{2}$$

In this context, the symbol  $P_m$  refers to the structural properties of the metal concerning the FG shell. As a result,  $P_m$  applies to the homogeneous cylindrical panel ( $\beta = 0$ ), while for the imperfect cylindrical panel ( $\beta < 1$ ), different values of  $P_m$  maybe relevant.

### 3. Theoretical Analysis

The classical shell thin theory (CST) is employed in this study to calculate the motion equations for the nonlinear vibration features of FGM porous shells. The strain–displacement relations are shown as [46]:

$$\left(\varepsilon_x \quad \varepsilon_y \quad \gamma_{xy}\right) = \left(\varepsilon_x^\circ \quad \varepsilon_y^\circ \quad \gamma_{xy}^\circ\right) - z\left(\lambda_x \quad \lambda_y \quad 2\lambda_{xy}\right), \tag{3}$$

With

$$\begin{aligned} \left( \varepsilon_x^\circ \quad \varepsilon_y^\circ \quad \gamma_{xy}^\circ \right) &= \left( \frac{\partial u}{\partial x} + \frac{1}{2} \left( \frac{\partial w}{\partial x} \right)^2 \quad \frac{\partial v}{\partial y} - \frac{w}{R} + \frac{1}{2} \left( \frac{\partial w}{\partial x} \right)^2 \quad \frac{\partial u}{\partial y} + \frac{\partial v}{\partial x} + \frac{\partial w}{\partial x} \frac{\partial w}{\partial y} \right) \\ \left( \lambda_x \quad \lambda_y \quad 2\lambda_{xy} \right) &= \left( \frac{\partial^2 w}{\partial x^2} \quad \frac{\partial^2 w}{\partial y^2} \quad \frac{\partial^2 w}{\partial x \partial y} \right) \end{aligned} \quad (4)$$

In which  $(\gamma_{xy}^\circ)$  is the shear strain and  $(\varepsilon_x^\circ, \varepsilon_y^\circ)$  are the normal strain at the middle surface panel. Deformations must resemble the compatibility equation. [47]:

$$\frac{\partial^2 \varepsilon_x^\circ}{\partial x^2} + \frac{\partial^2 \varepsilon_y^\circ}{\partial y^2} - \frac{\partial^2 \gamma_{xy}^\circ}{\partial x \partial y} = \left[ \frac{\partial^2 w}{\partial x \partial y} \right]^2 - \frac{\partial^2 w}{\partial x^2} \frac{\partial^2 w}{\partial y^2} - \frac{1}{R} \frac{\partial^2 w}{\partial x^2}, \quad (5)$$

The stress-strain relationships for the cylindrical FGM panel can be obtained as [48]:

$$\begin{aligned} \sigma_x &= \frac{E(z)}{1-\nu^2} (\varepsilon_x + \nu \varepsilon_y), \\ \sigma_y &= \frac{E(z)}{1-\nu^2} (\varepsilon_y + \nu \varepsilon_x), \\ \tau_{xy} &= \frac{E(z)}{2(1+\nu)} \gamma_{xy}, \end{aligned} \quad (6)$$

These are the internal forces and moments, respectively [49]:

$$\begin{aligned} (N_x, N_y, N_{xy}) &= \int_{-h/2}^{h/2} (\sigma_x^{sh}, \sigma_y^{sh}, \tau_{xy}^{sh}) dz, \\ (M_x, M_y, M_{xy}) &= \int_{-h/2}^{h/2} (\sigma_x^{sh}, \sigma_y^{sh}, \tau_{xy}^{sh}) z dz, \end{aligned} \quad (7)$$

The following form describes the non-linear motion equations of an FGM cylindrical panel based on CST [50], and the assumes [51]  $u \ll w$ , and  $v \ll w$ , leads to  $\rho_1 \frac{\partial^2 u}{\partial t^2} = 0, \rho_1 \frac{\partial^2 v}{\partial t^2} = 0$ :

$$\begin{aligned} \delta u: \frac{\partial N_x}{\partial x} + \frac{\partial N_{xy}}{\partial y} &= 0, \\ \delta v: \frac{\partial N_{xy}}{\partial x} + \frac{\partial N_y}{\partial y} &= 0, \\ \delta w: \frac{\partial^2 M_x}{\partial x^2} + 2 \frac{\partial^2 M_{xy}}{\partial x \partial y} + \frac{\partial^2 M_y}{\partial y^2} + N_x \frac{\partial^2 w}{\partial x^2} + 2 N_{xy} \frac{\partial^2 w}{\partial x \partial y} + \\ N_y \frac{\partial^2 w}{\partial y^2} + q + \frac{N_y}{R} &= \rho_1 \frac{\partial^2 w}{\partial t^2}, \end{aligned} \quad (8)$$

The stress function is used to determine the first two variables in the format shown below [52]:

$$N_x = \frac{\partial^2 f}{\partial y^2}, N_y = \frac{\partial^2 f}{\partial x^2}, N_{xy} = -\frac{\partial^2 f}{\partial x \partial y}, \tag{9}$$

Substituting equations 3, 6, and 7 into equations 5 and 8, taking into account equations 4 and 9, we obtain the following results:

$$\begin{aligned} &A_{11} \frac{\partial^4 f}{\partial x^4} + (A_{66} - 2A_{12}) \frac{\partial^4 f}{\partial x^2 \partial y^2} + A_{22} \frac{\partial^4 f}{\partial y^4} + B_{21} \frac{\partial^4 w}{\partial x^4} \\ &+ (B_{11} + B_{22} - 2B_{66}) \frac{\partial^4 w}{\partial x^2 \partial y^2} + B_{12} \frac{\partial^4 w}{\partial y^4} + \frac{1}{R} \frac{\partial^2 w}{\partial x^2} \\ &= \left( \frac{\partial^2 w}{\partial x \partial y} \right)^2 - \frac{\partial^2 w}{\partial x^2} \frac{\partial^2 w}{\partial y^2}, \end{aligned} \tag{10}$$

$$\begin{aligned} &\rho_1 \frac{\partial^2 w}{\partial t^2} + D_{11} \frac{\partial^4 w}{\partial x^4} + (D_{12} + D_{21} + 4D_{66}) \frac{\partial^4 w}{\partial x^2 \partial y^2} + D_{22} \frac{\partial^4 w}{\partial y^4} \\ &- B_{21} \frac{\partial^4 f}{\partial x^4} - (B_{11} + B_{22} - 2B_{66}) \frac{\partial^4 f}{\partial x^2 \partial y^2} - B_{12} \frac{\partial^4 f}{\partial y^4} - \frac{1}{R} \frac{\partial^2 f}{\partial x^2} \\ &- \frac{\partial^2 f}{\partial y^2} \frac{\partial^2 w}{\partial x^2} + 2 \frac{\partial^2 f}{\partial x \partial y} \frac{\partial^2 w}{\partial x \partial y} - \frac{\partial^2 f}{\partial x^2} \frac{\partial^2 w}{\partial y^2} = q, \end{aligned} \tag{11}$$

The coefficients are demonstrated in the Appendix. The two aforementioned equations (10 and 11) are used to evaluate how the non-linear vibration response of the porous cylindrical panels behaves.

#### 4. Solution Method

For the porous FG sandwich cylindrical panel exposed to an evenly distributed load ( $q_0$ ), the following simply supported boundary conditions (SSSS) for all edges of shell are employed in this paper [53]:

$$\begin{aligned} &w = 0, M_x = 0, u = 0, \text{ at } x = 0, a, \\ &w = 0, M_y = 0, v = 0, \text{ at } y = 0, b, \end{aligned} \tag{12}$$

The cited conditions (12) can be accomplished if the mode shape is determined by:

$$w = W(t) \sin\left(\frac{m\pi x}{a}\right) \sin\left(\frac{n\pi y}{b}\right), \tag{13}$$

where, in the axial and circumferential directions, respectively,  $m, n=1, 2, \dots$  denotes the natural number of half-waves. Equation (10), in place of Equation (13), yields the following equation for the unknown in (f):

$$f(x, y, t) = A_1 \cos(2\lambda_m x) + A_2 \cos(2\delta_n y) + A_3 \sin(\lambda_m x) \sin(\delta_n y), \tag{14}$$

where  $\lambda_m = \frac{m\pi}{a}, \delta_n = \frac{n\pi}{b}$ , and ( $A_1, A_2,$  and  $A_3$ ) are defined in the Appendix. Equation (11) is replaced by Equations (13 & 14). Subsequently, we solve this equation by employing Galerkin's technique as follows:

$$M\ddot{W} + \left(D + \frac{B^2}{A}\right)W + \frac{8mn\lambda^2 B}{3\pi^2 A} \delta_1 \delta_2 W^2 + HW^2 + KW^3 - \frac{4qa^4}{mn\pi^6} \delta_1 \delta_2 = 0, \tag{15}$$

All coefficients in Eq. 15 are shown in the appendix. The nonlinear behavior of cylindrical panels formed of single-phase metal porous FG is studied and analyzed using the aforementioned equation. When the cylindrical sandwich shell panel is exposed to an evenly distributed stress [ $q = Q \sin \Omega t$ ], the equation of non-linear (15) becomes as follows:

$$M\ddot{W} + \left( D + \frac{B^2}{A} \right) W + \frac{8mn\lambda^2 B}{3\pi^2 A} \delta_1 \delta_2 W^2 + HW^2 + KW^3 - \frac{4a^4}{mn\pi^6} \delta_1 \delta_2 Q \sin \Omega t = 0, \quad (16)$$

Using the Runge-Kutta method to solve the aforementioned equation with initial conditions  $W(0) = 0$ , it is possible to calculate the responses of porous FGM panels. The vibration equation is free and linear. (16) results in:

$$M\ddot{W} + \left( D + \frac{B^2}{A} \right) W = 0, \quad (17)$$

The following formula may be used to determine the linear natural frequencies of cylindrical porous FG panels:

$$\omega_L = \sqrt{\frac{1}{M} \left( D + \frac{B^2}{A} \right)}, \quad (18)$$

## 5. Results and Discussion

This section focusses on presenting numerical vibration examples of cylindrical shells made of functionally graded materials. The aim is to analyse and discuss the free vibration behaviour of the FGM sandwich shell by changing different parameters such as geometries, porosity, various metal cores, face sheets, and gradient index. Firstly, the findings of the current study of non-dimensional natural frequencies  $\tilde{\omega} = \omega_L h \sqrt{\frac{\rho_c}{E_c}}$  The comparison will be with those of Duc [54] based on classical shell theory (CST), Alijani et al. [55] according to Donnell's non-linear shell theory and Matsunaga [56] based on (2D) higher order theory. Good agreements are obtained in this comparison, as shown in Table 1, which is an excellent example of this. Sandwich cylindrical shell panels made of polyethylene are widely used in various engineering applications such as aerospace, automobile, and naval industries due to their superior mechanical properties and lightweight characteristics [57]. However, the presence of porosity within these panels can significantly affect their non-linear dynamic behaviour, which can have implications for their performance and reliability. Material properties employed in the current analysis are provided in Table 2.

**Table 1:** Comparison of the Non-Linear Natural Frequency Factor

a/R	N	Ref [54]	Ref [55]	Ref [56]	Present
<i>FGM cylindrical panel</i> 0.5	0	0.0624	0.0648	0.0622	0.0648
	0.5	0.0528	0.0553	0.0535	0.0553
	1	0.0494	0.0501	0.0485	0.0501
	4	0.0407	0.0430	0.0413	0.0430
	10	0.0379	0.0408	0.0390	0.0409

**Table 2:** Material characteristics of the FG sandwich cylindrical shell parts

Material	E (MPa)	$\rho$ (Kg/m <sup>3</sup> )	$\nu$	Ref.
<i>Polyethylene</i>	1100	950	0.42	[57]
<i>PEEK - 30 % CF</i>	7700	1410	0.44	[58]
<i>PEEK - 30 % GF</i>	6300	1510	0.34	[57]
<i>PEEK -1000 Natural</i>	4400	1310	0.40	[57]
<i>Aluminium</i>	70,000	2702	0.3	[57]

The sandwich cylindrical shells have three values of the porosity factor  $\beta$  (0.1, 0.2, and 0.3),  $a = b = 0.5$  m, radius of curvature = 3 m, and a volume fraction exponent  $k$  ranging from 0.5 to 10. The height of the porous metal core ranges from 10 to 20 mm, while the skin height ranges from 1 to 2.5 mm. Table 3 presents the analytical findings of the natural frequencies parameter for a sandwich single-phase polyethylene FG shell. The investigation reveals that the frequency parameter of the sandwich FGM cylindrical shell increases as the porous parameter rises, but decreases as the gradient index increases. This can be attributed to the decrease in material rigidity caused by the increase in the gradient index. In this case, a higher gradient index indicates a more significant variation in material composition, leading to non-uniformity in stiffness across the shell's thickness. This nonuniformity results in a reduction in the natural frequency of the cylindrical shell.

**Table 3:** The natural frequency ( $\omega$ ) of the cylindrical sandwich shell with a polyethylene FGM core and a face sheet thickness of 1 mm

Thickness mm	Power law	porosity coefficient %		
		10	20	30
10	0.5	256.0382	261.6831	267.7401
	1	254.6791	258.7978	263.1347
	5	252.0176	253.2948	254.5932
20	0.5	372.1520	382.1790	393.1320
	1	369.7514	377.0082	384.7468
	5	365.0619	367.2380	369.4586

The results in Figure 2 show how the natural frequency is affected by the type of porous metal used, with a porosity ratio of 10, 20, and 30%. The metals tested were polyethylene, PEEK-30% CF, PEEK-30% GF, and PEEK-1000 Natural, with a core thickness of 10mm, face sheet thickness of 1mm, and material gradient of 0.5. The analysis revealed that polyurethane exhibited greater stiffness compared to PEEK-1000 Natural and all types of PEEK due to its superior mechanical properties. This is because polyurethane is less dense and more compliant than PEEK, which means that it can vibrate or oscillate more quickly when subjected to external forces. Additionally, the molecular structure of polyurethane is more flexible than that of PEEK, which also contributes to its higher natural frequency.

Figures 3-6 represent the nonlinear dynamic response of the sandwich shell FG with various metal cores, namely polyethylene, PEEK-30% CF, PEEK-30% GF and PEEK-1000 Natural, respectively, with porosity values of 10%, 30% and 50%. The material gradient is 0.5, the FG single-phase thickness is 10 mm, and the face sheet layer is 1 mm. The excitation force is  $q = 1000 \sin 800 t$ . The results showed that increasing the porosity parameter leads to a decrease in the time deflection curve for all types of metals used. This is because porosity affects the mechanical properties of a metal, including its stiffness, strength, and damping properties, which can in turn affect its dynamic response. Furthermore, the damping properties of a material can also be affected by porosity. Damping refers to the ability of a material to absorb energy and dissipate it as heat, which can help to reduce vibrations and prevent damage.

Figure 7 shows the comparison between the metal cores used in this study concerning the amplitude of nonlinear vibration response at porosity 10%, hFG = 10mm, face sheet thickness = 1mm, and material gradient = 0.5. The curve showed that there is less deflection in PEEK-30% CF compared to other materials. As a result, it has a higher amplitude of the nonlinear vibration response, meaning that it undergoes greater deformation when subjected to a given force. PEEK-30% CF has a lower amplitude of non-linear vibration response compared to polyethylene, meaning that it undergoes less deformation when subjected to a given force. PEEK-30% GF has a slightly higher amplitude of nonlinear vibration response compared to PEEK-30% CF.

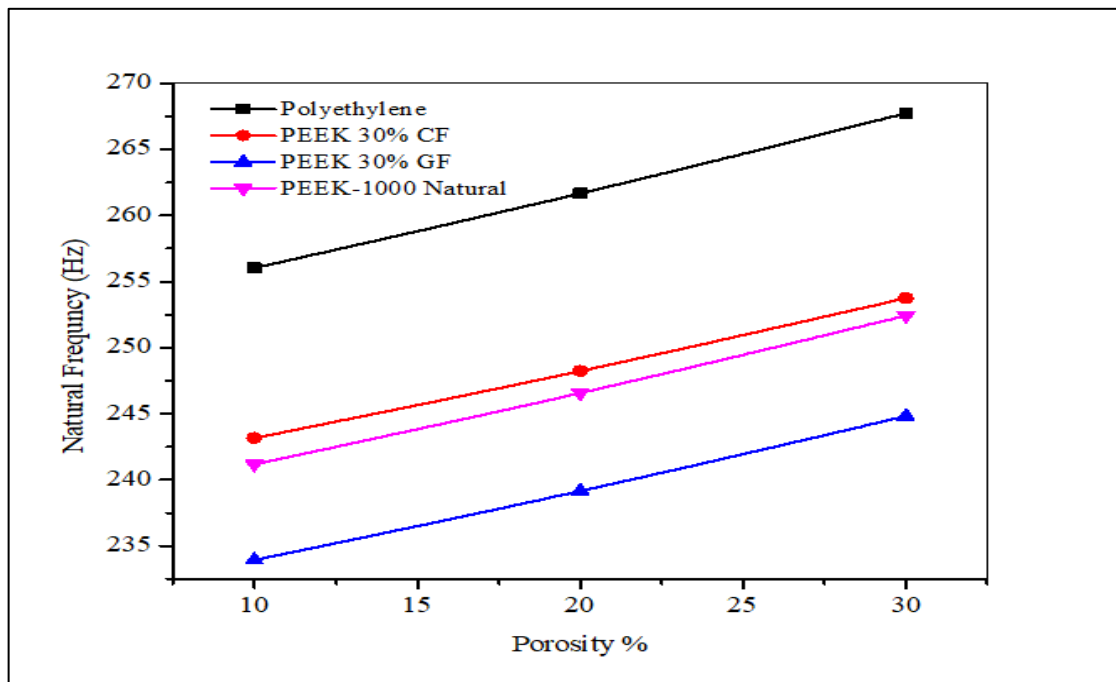


**Figure 2:** Results of the fundamental natural frequency for different porous metals of sandwich cylindrical shell panel

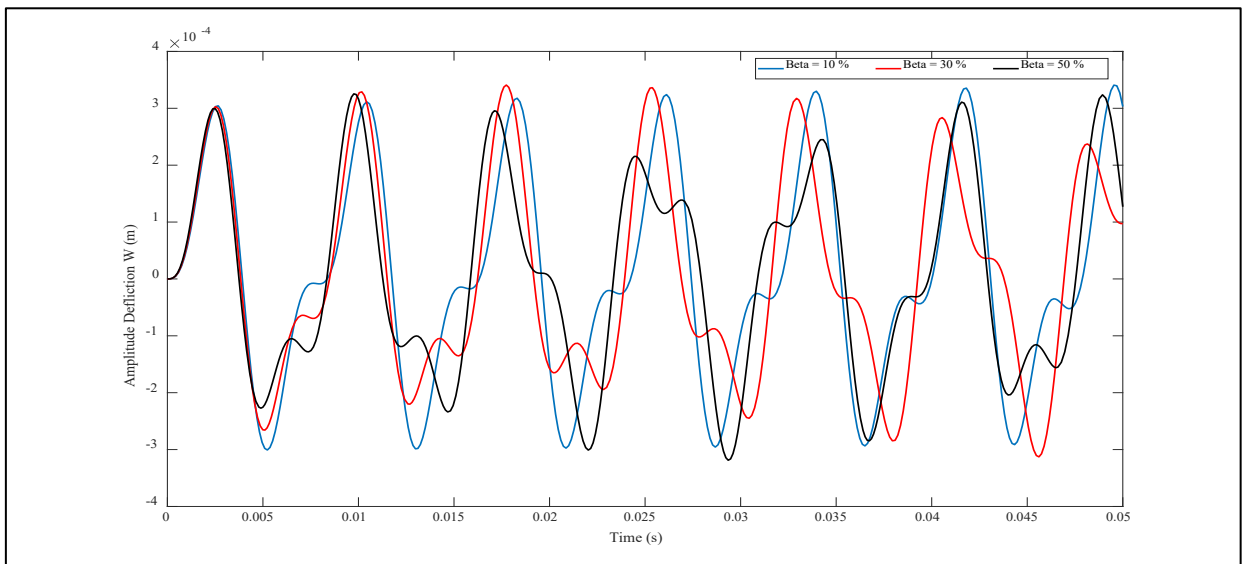


**Figure 3:** Impacts of increasing porosity on the nonlinear dynamic behavior of polyethylene sandwich cylindrical shell panels

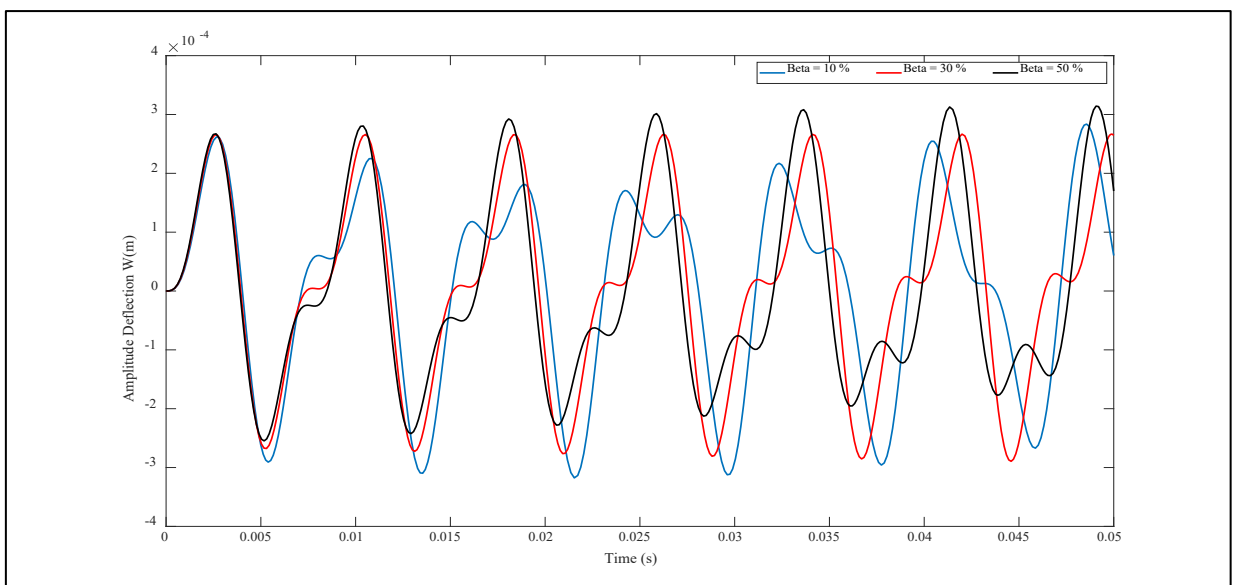


**Figure 4:** Results of rising porosity on the dynamic characteristics of PEEK-30% CF sandwich cylindrical shell panels

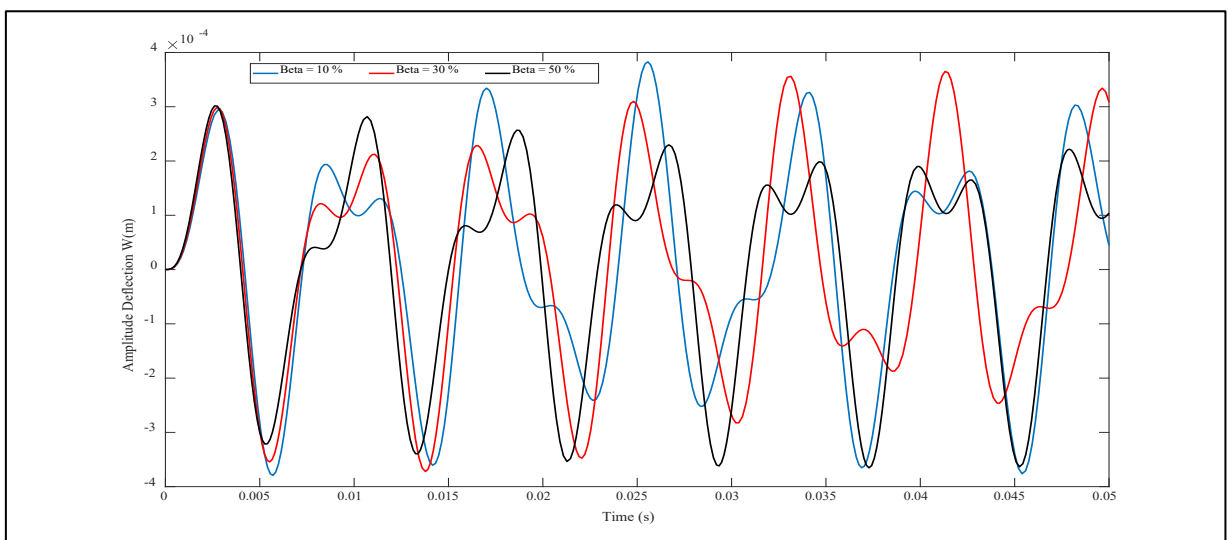


**Figure 5:** Results of rising porosity on the dynamic characteristics of PEEK - 30 % GF sandwich cylindrical shell panels



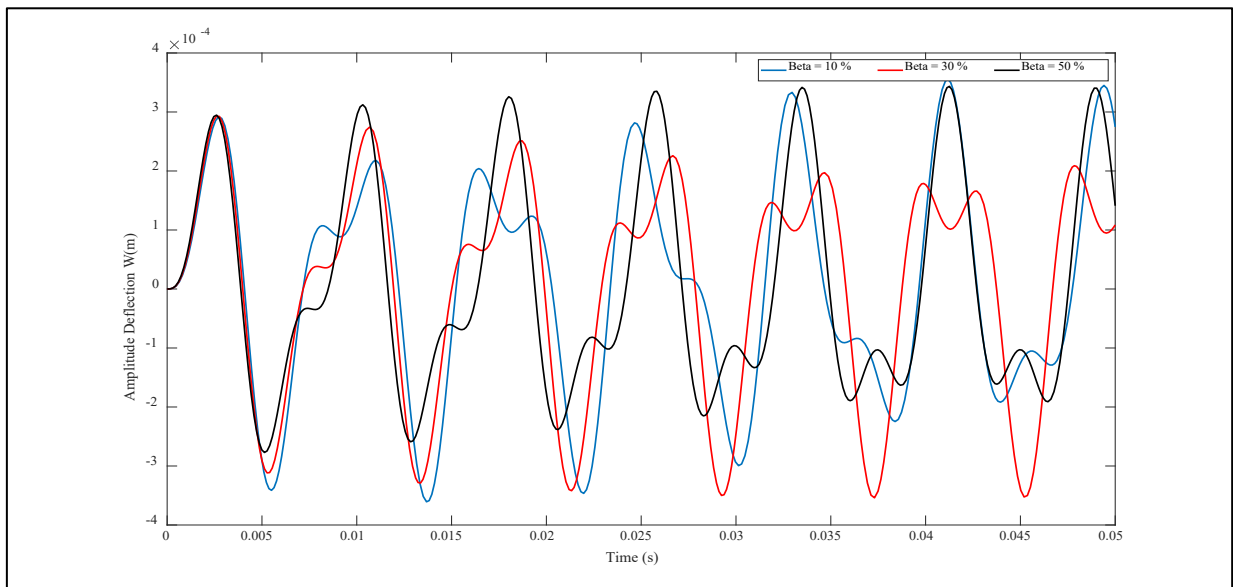


**Figure 6:** Effect of the porosity parameter on the time-deflection curve of PEEK-1000 natural sandwich cylindrical shell Panels

Figure 7 shows the comparison between the metal cores (polyethylene, PEEK-30% CF, PEEK-30% GF, and PEEK-1000 Natural) used in this study concerning the amplitude of the nonlinear vibration response at porosity 10%, hFG = 10mm, thickness of the face sheet = 1mm, and material gradient = 0.5. The curve showed that less deflection occurs in PEEK-30% GF compared to other materials. As a result, it has a higher amplitude of the nonlinear vibration response, meaning that it undergoes greater deformation when subjected to a given force. PEEK-30% GF has a lower amplitude of nonlinear vibration response compared to polyethylene, meaning that it undergoes less deformation when subjected to a given force. PEEK-30% CF has a slightly higher amplitude of nonlinear vibration response compared to PEEK-30% GF. PEEK-1000 Natural has a higher amplitude of nonlinear vibration response compared to PEEK-30% CF and PEEK-30% GF due to its lower stiffness.

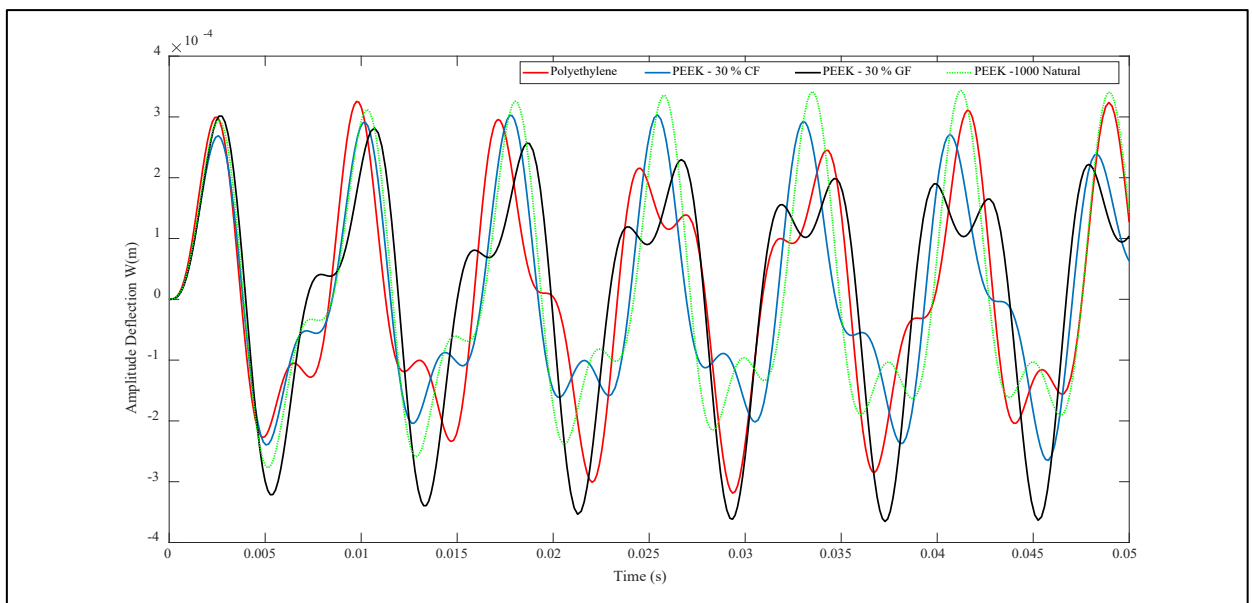


**Figure 7:** Dynamic behaviour of cylindrical panels of FGM sandwich with different porous metal cores

The natural frequency of single phase FG sandwich cylindrical shells at a porous factor of 10% was analysed in Figure 8 for different power law indexes ( $k=0.5, 1, 5,$  and  $10$ ) and various metal cores, with a core height of 10mm and 1mm face sheets. The findings reveal that as the power-law index increases, the natural frequency values decrease in all metal cores. This is attributed to the reduction in bending rigidity and elasticity modulus of the cylindrical shell, leading to decreased material strength. Based on the analysis, it can be observed that the Polyethylene core exhibits a greater natural frequency compared to other types of cores. This is because of its superior mechanical properties values.

Figure 9 illustrates the effect of the material gradient on the nonlinear dynamic behavior of porous FG single-phase sandwich cylindrical panels. The results show that an increase in the power law index indicates an increase in the rate of deformation of a material under a given stress or load. Therefore, the time-displacement curve is expected to increase with the rise of the power-

law index. This is because a higher power-law index indicates that the material will deform more rapidly under the applied load, resulting in a more rapid increase in displacement over time. Conversely, a lower power-law index indicates that the material will deform more slowly under the applied load, resulting in a slower increase in displacement over time.

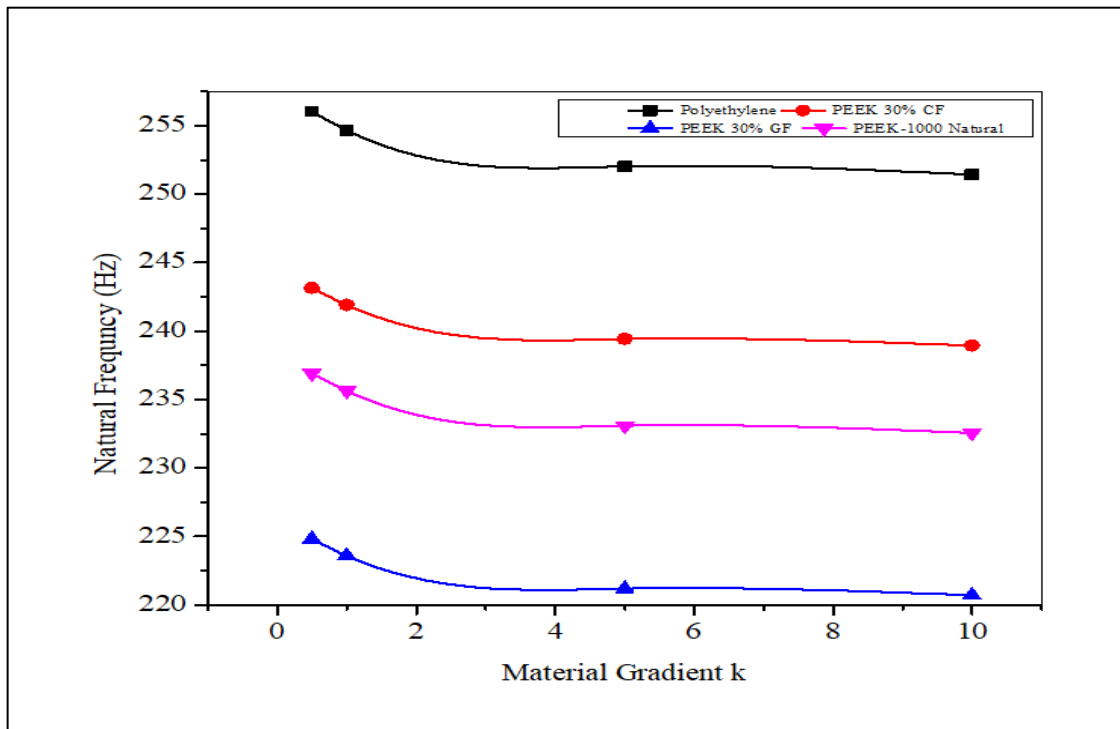


Figure 8: Effect volume fraction index on the natural frequency parameter of a sandwich FGM shell with various porous metal core

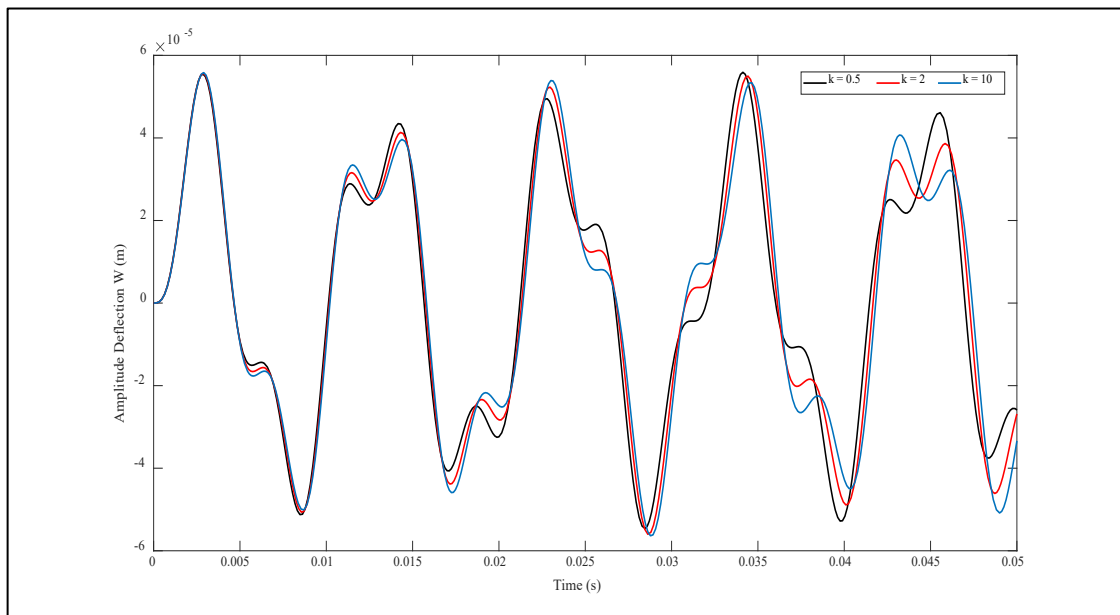


Figure 9: Effect of the power law index on the time-deflection curve of porous FG single-phase sandwich cylindrical panels

The graphs in Figures 10-13 show how changing the FG single-phase core thickness and face sheet affects the natural frequency and nonlinear amplitude deflection of simply supported cylindrical panels with different porous metal cores. The dimensions of the shell are  $a=b=0.5$ ,  $R=3$  m, with a power law index of 0.5 and a porosity coefficient of 10%. The thickness of the FGM core ranges from 10 to 20 mm, while the thickness of the face sheet ranges from 1 to 2.5mm. The graph indicates that increasing the thickness of the FGM core or face sheet leads to a significant increase in the natural frequency of the sandwich shells in all types of metal core. These results suggest that increasing the thickness of either component strengthens the stiffness of the FG sandwich cylindrical shell. This is because a stiffer structure will resist deformation more effectively and require more energy to deform, resulting in a higher natural frequency. However, a stiffer structure also means that it will have a higher

deflection amplitude under the same applied load. This is because the structure will require a greater force to deform, and once it does deform, the deformation will be more pronounced due to the increased stiffness of the structure. This is a result of the increased stiffness of the sandwich structure, which affects both its natural frequency and deformation behavior.

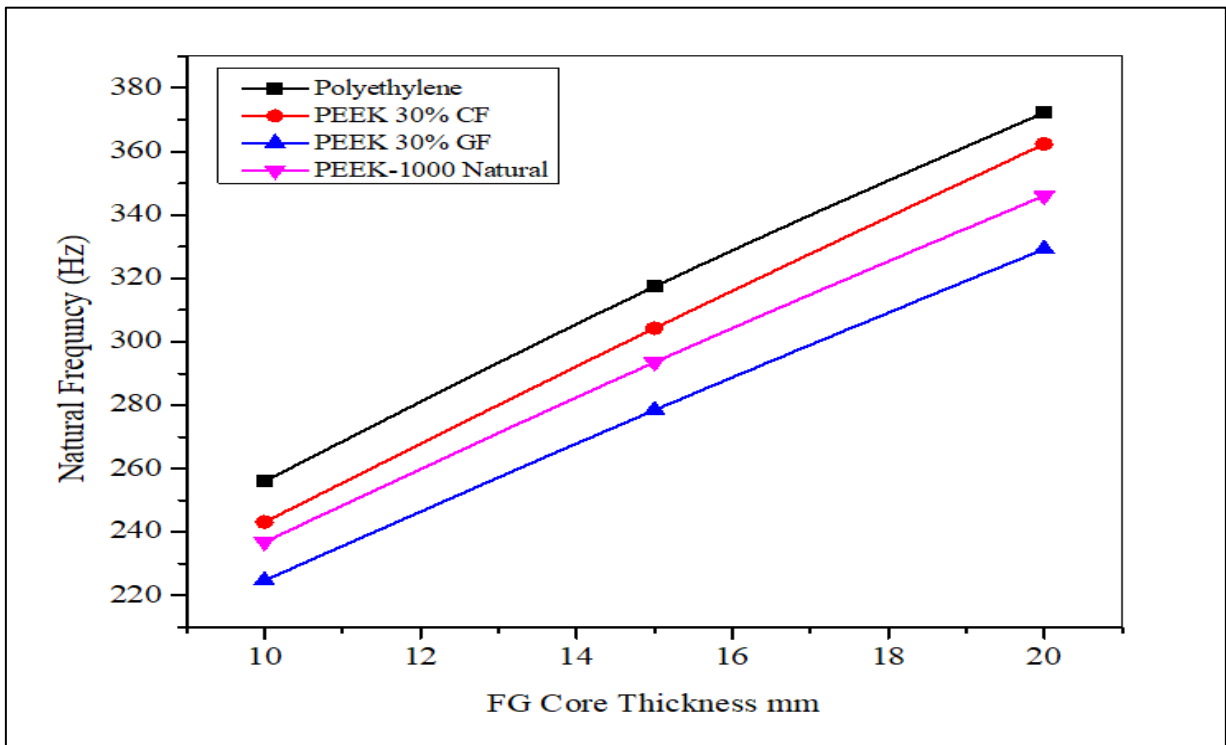


Figure 10: Results of the natural frequency for different FGM cores with face sheet thicknesses of 1 mm

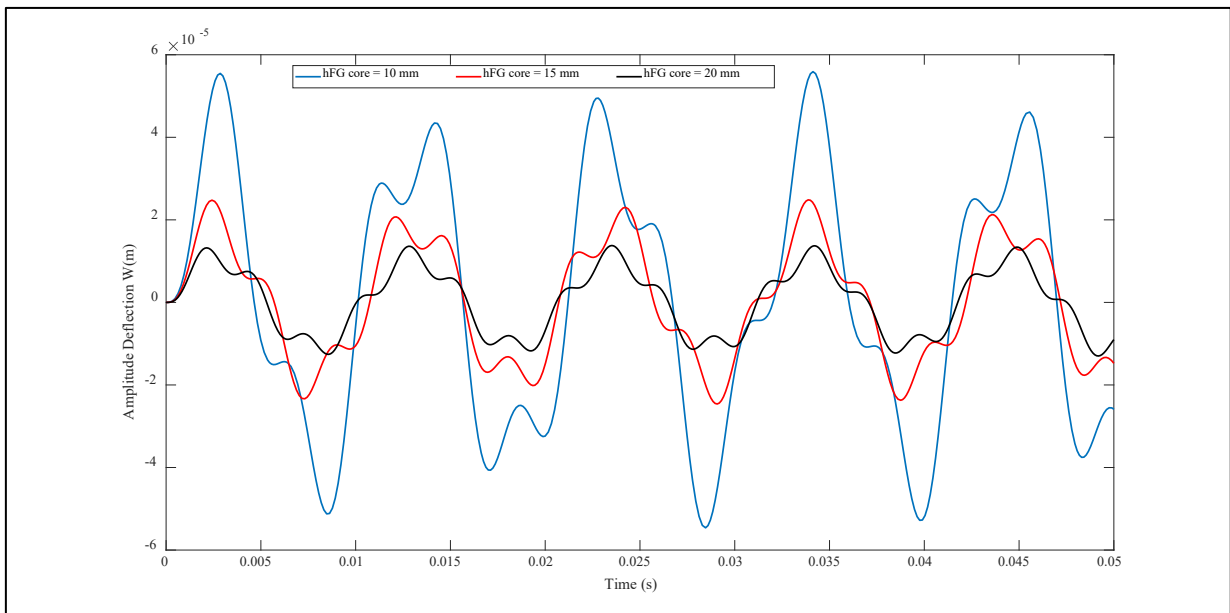


Figure 11: Result of the FG core thickness on the non-linear dynamic response of porous FG single-phase sandwich shells

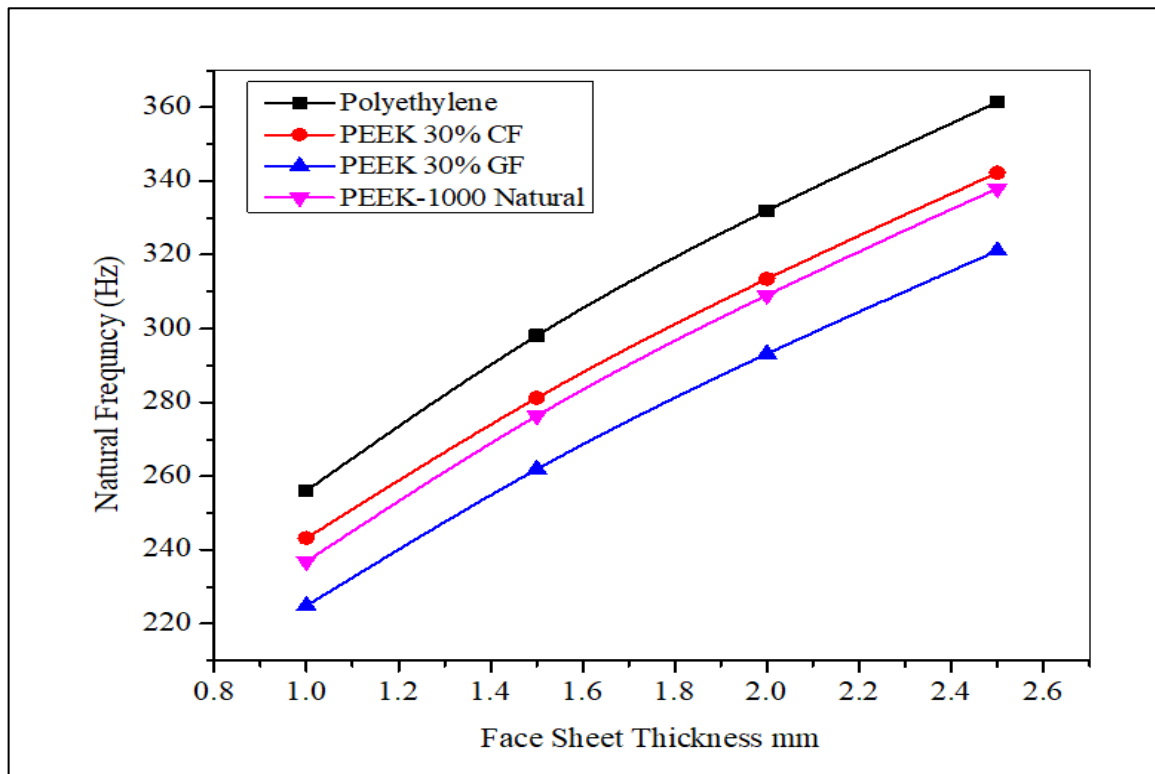


Figure 12: Results of the natural frequency for different face sheet thicknesses with FGM cores 10 mm

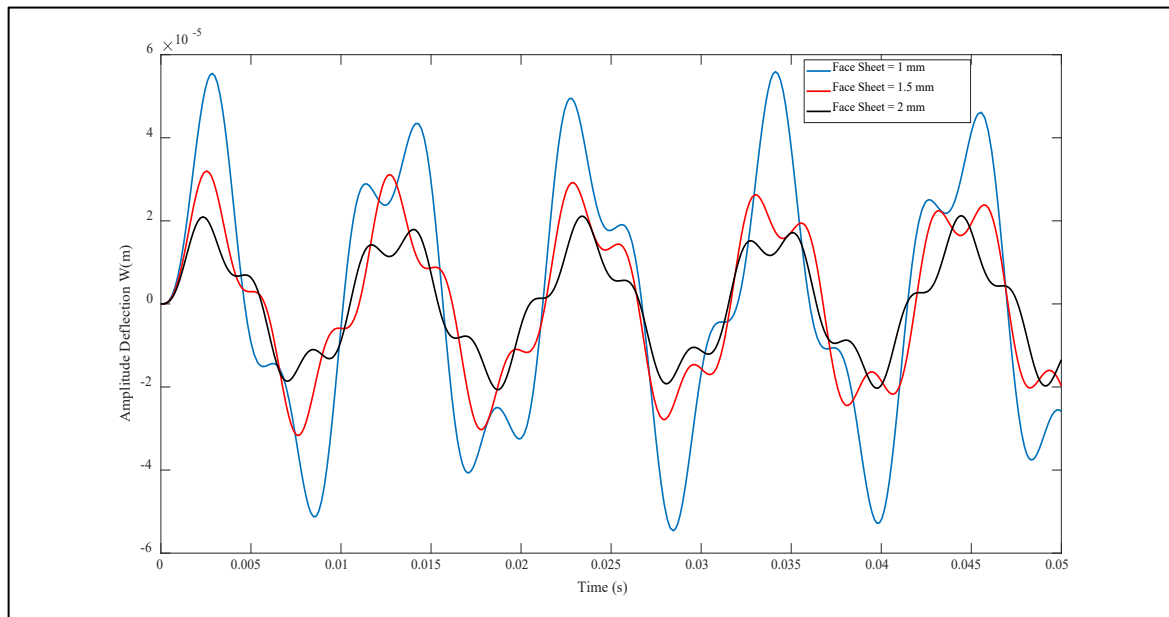


Figure 13: Result of the thickness of the face sheet on the non-linear dynamic response of porous FG single-phase sandwich shells

## 6. Conclusion

The non-linear vibration dynamic response of a functionally graded sandwich cylindrical shell panel is proposed to be analytically examined in this study. The cylindrical sandwich panels are made up of a core composed of a single phase porous metal, such as polyethylene, PEEK-30% CF, PEEK-30% GF, or PEEK-1000 natural. The core is attached to homogeneous skins on both sides using an appropriate adhesive. The formulas utilise geometric non-linearity and are based on the CST. Runge-Kutta techniques are applied to solve the nonlinear equations. The results of some studies were compared with those of other authors. The study discussed in the paper investigates how different factors affect the free vibration properties of functionally graded sandwich shells. These factors include porosity, gradient index, and thickness of the FG core and face sheets. The metal cores used in this study show different amplitudes of non-linear vibration response depending on their stiffness and strength. Polyethylene has the highest amplitude of nonlinear vibration response due to its lower stiffness, while PEEK-30% GF has the lowest amplitude of nonlinear vibration response due to its high stiffness and strength. PEEK-30% CF and PEEK-1000 Natural

have intermediate amplitudes of nonlinear vibration response due to their lower stiffness compared to PEEK-30% GF..As a result, by changing these factors, we can effectively regulate the porous FGM cylindrical shells' vibration and dynamic response.

## Appendix

$$\begin{aligned}
 I_{10} &= \frac{E_1}{1-\nu^2}, I_{20} = \frac{\nu E_1}{1-\nu^2}, I_{30} = \frac{E_1}{2(1+\nu)}, I_{11} = \frac{E_2}{1-\nu^2}, \\
 I_{21} &= \frac{\nu E_2}{1-\nu^2}, I_{31} = \frac{E_2}{2(1+\nu)}, I_{12} = \frac{E_3}{1-\nu^2}, I_{22} = \frac{\nu E_3}{1-\nu^2}, \\
 I_{32} &= \frac{E_3}{2(1+\nu)}, A_{11} = \frac{I_{10}}{\Delta}, A_{22} = \frac{I_{10}}{\Delta}, A_{12} = \frac{I_{20}}{\Delta}, A_{66} = \frac{1}{I_{30}}, \Delta = (I_{10})(I_{10}) - I_{20}^2, \\
 E_i &= \left\{ \begin{aligned} &\int_{\frac{(h_{FG})}{2}}^{\frac{(h_{FG})}{2}} E(z) dz + \int_{\frac{(h_{FG})}{2}}^{\frac{(h_{FG})}{2}} \left[ E_m - \beta \cdot E_m \left( \frac{z}{h} + \frac{1}{2} \right)^k \right] dz \\ &+ \int_{\frac{(h_{FG})}{2}}^{\frac{(h_{FG}+h_U)}{2}} E(z) dz \end{aligned} \right\} (1, z, z^2), \\
 \rho_1 &= \int_{\frac{(h_{FG})}{2}}^{\frac{(h_{FG})}{2}} \rho(z) dz + \int_{\frac{(h_{FG})}{2}}^{\frac{(h_{FG})}{2}} \left[ \rho_m - \beta \cdot \rho_m \left( \frac{z}{h} + \frac{1}{2} \right)^k \right] dz \\
 &+ \int_{\frac{(h_{FG})}{2}}^{\frac{(h_{FG}+h_U)}{2}} \rho(z) dz, \\
 A_{11} &= \frac{I_{10}}{\Delta}, A_{22} = \frac{I_{10}}{\Delta}, A_{12} = \frac{I_{20}}{\Delta}, A_{66} = \frac{1}{I_{30}}, \Delta = (I_{10})(I_{10}) - I_{20}^2, \\
 B_{11} &= A_{22}I_{11} - A_{12}I_{21}, B_{22} = A_{11}I_{11} - A_{12}I_{21}, \\
 B_{12} &= A_{22}I_{21} - A_{12}I_{11}, B_{21} = A_{11}I_{21} - A_{12}I_{11}, B_{66} = \frac{I_{31}}{I_{30}}, \\
 D_{11} &= I_{12} - B_{11}B_{12} - I_{21}B_{21}, D_{22} = I_{22} - B_{22}I_{11} - I_{21}B_{12}, \\
 D_{12} &= I_{22} - B_{12}I_{11} - I_{21}B_{22}, D_{21} = I_{22} - B_{21}I_{11} - I_{21}B_{11}, \\
 D_{66} &= I_{32} - I_{31}B_{66}, M = \frac{a^4}{\pi^4} \rho_1, \\
 A &= A_{11}m^4 + (A_{66} - 2A_{12})m^2n^2\lambda^2 + A_{22}n^4\lambda^4, \\
 B &= B_{21}m^4 + (B_{11} + B_{22} - 2B_{66})m^2n^2\lambda^2 + B_{12}n^4\lambda^4 - \frac{a^2}{\pi^2} \frac{1}{R} m^2, \\
 D &= D_{11}m^4 + (D_{12} + D_{21} + 4D_{66})m^2n^2\lambda^2 + D_{22}n^4\lambda^4, \\
 H &= \left[ \frac{2mn\lambda^2}{3\pi^2} \left( \frac{B_{21}}{A_{11}} + \frac{B_{12}}{A_{22}} \right) - \frac{a^2}{6\pi^4 mn} \frac{n^2\lambda^2}{A_{11}} \frac{1}{R} \right] \delta_1 \delta_2, \\
 K &= \frac{1}{16} \left( \frac{m^4}{A_{22}} + \frac{n^4\lambda^4}{A_{11}} \right), \lambda = \frac{a}{b}, \delta_1 = (-1)^m - 1, \delta_2 = (-1)^n - 1, \\
 A_1 &= \frac{n^2\lambda^2}{32A_{11}m^2} W^2, A_2 = \frac{m^2}{32A_{22}n^2\lambda^2} W^2, \\
 A_3 &= \frac{(B_{21}m^4 + (B_{11} + B_{22} - 2B_{66})m^2n^2\lambda^2 + B_{12}n^4\lambda^4 - \frac{a^2}{\pi^2} \frac{1}{R} m^2)}{(\Gamma_{11}m^4 + (A_{66} - 2A_{12})m^2n^2\lambda^2 + A_{22}n^4\lambda^4)} W,
 \end{aligned}$$

### Author contributions

Conceptualization, A. Mouthanna, S. Bakhy, and M. Al-Waily; formal analysis, A. Mouthanna, S. Bakhy, and M. Al-Waily; resources, A. Mouthanna, S. Bakhy, and M. Al-Waily. All authors have read and agreed to the published version of the manuscript.

### Funding

This research received no specific grant from any funding agency in the public, commercial, or not-for-profit sectors.

### Data availability statement

The data that support the findings of this study are available on request from the corresponding author.

### Conflicts of interest

The authors declare that there is no conflict of interest.

### References

- [1] A. Gupta, M. Talha, and B. N. Singh, Vibration characteristics of functionally graded material plate with various boundary constraints using higher order shear deformation theory, *Compos. B. Eng.*, 94 (2016) 64–74. <https://doi.org/10.1016/j.compositesb.2016.03.006>
- [2] S. M. Chorfi ,A. Houmat, Non-linear free vibration of a functionally graded doubly-curved shallow shell of elliptical plan-form, *Compos. Struct.*, 92 (2010) 2573–2581. <https://doi.org/10.1016/j.compstruct.2010.02.001>
- [3] E. K. Njim, S. H. Bakhy, and M. Al-Waily, Free vibration analysis of imperfect functionally graded sandwich plates: Analytical and experimental investigation, *Arch. Mater. Sci. Eng.*, 111 (2021) 49–65. <https://doi.org/10.5604/01.3001.0015.5805>
- [4] M. Srivastava, S. Maheshwari, and T. K. Kundra, Virtual Modelling and Simulation of Functionally Graded Material Component using FDM Technique, *Mater. Today. Proc.*, 2 (2015) 3471–3480. <https://doi.org/10.1016/j.matpr.2015.07.323>
- [5] D. T. Luat, D. Van Thom, T. T. Thanh, P. Van Minh, T. Van Ke, and P. Van Vinh, Mechanical analysis of bi-functionally graded sandwich nanobeams, *Adv. Nano. Res.*, 11 (2021) 55–71. <https://doi.org/10.12989/anr.2021.11.1.055>
- [6] V. T. Do, V. V. Pham, and H. N. Nguyen, On the Development of Refined Plate Theory for Static Bending Behavior of Functionally Graded Plates, *Math. Probl. Eng.*, 2020 (2020) 13. <https://doi.org/10.1155/2020/2836763>
- [7] S. A. Deepak and R. A. Shetty, Static and free vibration analysis of functionally graded rectangular plates using ANSYS, *Mater. Today. Proc.*, 45 (2021) 415–419. <https://doi.org/10.1016/j.matpr.2020.12.761>
- [8] A. K. Gantayat, M. K. Sutar, and J. R. Mohanty, Dynamic characteristic of graphene reinforced axial functionally graded beam using finite element analysis, *Mater. Today. Proc.*, 62 (2022) 5923–5927. <https://doi.org/10.1016/j.matpr.2022.04.636>
- [9] D. Van Thom, D. Hong Duc, P. Van Minh, and N. Son Tung, Finite Element Modelling For Vibration Response Of Cracked Stiffened Fgm Plates, *Vietnam J. Sci. Technol.*, 58 (2020) 119–129.
- [10] T. , H. D. D. , C. T. N. , and D. D. N. Van Do, Thermal buckling analysis of cracked functionally graded plates, *Int. J. Struct. Stab. Dyn.*, 22 (2022) 2250089. <https://doi.org/10.1142/S0219455422500894>
- [11] A. Karakoti, S. Pandey, and V. Ranjan Kar, Bending analysis of sandwich shell panels with exponentially graded core, *Mater. Today: Proc.*, 28 (2020) 1706–1708. <https://doi.org/10.1016/j.matpr.2020.05.132>
- [12] N. Hassan Hadi , K. Aziz Ameen, Geometrically Nonlinear Free Vibration Analysis of Cylindrical Shells Using high Order Shear Deformation Theory-A Finite Element Approach, *Eng. Technol. J.*, 29 (2011) 2156- 2174.
- [13] M. J. Jweeg, A. D. Mohammed, and M. AAlshamari, Theoretical and Experimental Investigations of Vibration Characteristics of a Combined Composite Cylindrical-Conical Shell Structure, *Eng. Technol. J.*, 28 (2010) 7011-7026.
- [14] S. Medjmadj, A. Si Salem, and S. Ait Taleb, Experimental behavior of plaster/cork functionally graded core sandwich panels with polymer skins, *Constr. Build. Mater.*, 344 (2022) 128257. <https://doi.org/10.1016/j.conbuildmat.2022.128257>
- [15] P. T. Dat, D. Van Thom, and D. T. Luat, Free vibration of functionally graded sandwich plates with stiffeners based on the third-order shear deformation theory, *Vietnam J. Mech.*, 38 (2016) 103–122. <https://doi.org/10.15625/0866-7136/38/2/6730>
- [16] P. H. Cong and N. D. Duc, Nonlinear thermo-mechanical analysis of ES double curved shallow auxetic honeycomb sandwich shells with temperature- dependent properties, *Compos. Struct.*, 279 (2022) 114739. <https://doi.org/10.1016/j.compstruct.2021.114739>
- [17] V. T. T. et al. Anh, Vibration of hybrid eccentrically stiffened sandwich auxetic double curved shallow shells in thermal environment, *Aerosp. Sci. Technol.*, 137 (2023) 108277. <https://doi.org/10.1016/j.compstruct.2021.114739>

- [18] S. Zghal, S. Trabelsi, A. Frikha, and F. Dammak, Thermal free vibration analysis of functionally graded plates and panels with an improved finite shell element, *J. Therm. Stresses*, 44 (2021) 315–341. <https://doi.org/10.1080/01495739.2021.1871577>
- [19] H. Ahmadi, A. Bayat, and N. D. Duc, Nonlinear forced vibrations analysis of imperfect stiffened FG doubly curved shallow shell in thermal environment using multiple scales method, *Compos. Struct.*, 256 (2021) 113090. <https://doi.org/10.1016/j.compstruct.2020.113090>
- [20] E. Njim, S. Bakhi, and M. Al-Waily, Experimental and Numerical Flexural Properties of Sandwich Structure with Functionally Graded Porous Materials, *Eng. Technol. J.*, 40 (2022) 137–147. <https://doi.org/10.30684/etj.v40i1.2184>
- [21] E. Kadum Njim, S. H. Bakhy, and M. Al-Waily, Analytical and numerical investigation of buckling load of functionally graded materials with porous metal of sandwich plate, *Mater. Today. Proc.*, 2021, <https://doi.org/10.1016/j.matpr.2021.03.557>
- [22] E. K. Njim, S. H. Bakhy, and M. Al-Waily, Optimisation design of functionally graded sandwich plate with porous metal core for buckling characterisations, *Pertanika J. Sci. Technol.*, 29 (2021) 3113–3141. <https://doi.org/10.47836/PJST.29.4.47>
- [23] E. Kadum Njim, S. H. Bakhy, and M. Al-Waily, Optimization design of vibration characterizations for functionally graded porous metal sandwich plate structure, *Mater. Today. Proc.*, 2021, <https://doi.org/10.1016/j.matpr.2021.03.235>
- [24] E. K. Njim, S. H. Bakhy, and M. Al-Waily, Analytical and numerical investigation of free vibration behavior for sandwich plate with functionally graded porous metal core, *Pertanika J. Sci. Technol.*, 29 (2021) 1655–1682. <https://doi.org/10.47836/pjst.29.3.39>
- [25] E. K. Njim, S. H. Bakhy, and M. Al-Waily, Analytical and numerical investigation of buckling behavior of functionally graded sandwich plate with porous core, *J. Appl. Sci. Eng.*, 25 (2022) 339–347. [https://doi.org/10.6180/jase.202204\\_25\(2\).0010](https://doi.org/10.6180/jase.202204_25(2).0010)
- [26] E. K. Njim, S. H. Bakhy, and M. Al-Waily, Analytical and numerical investigation of free vibration behavior for sandwich plate with functionally graded porous metal core, *Pertanika J. Sci. Technol.*, 29 (2021) 1655–1682. <https://doi.org/10.47836/pjst.29.3.39>
- [27] F. Ebrahimi, A. Dabbagh, and M. Taheri, Vibration analysis of porous metal foam plates rested on viscoelastic substrate, *Eng. Comput.*, 37 (2021) 3727–3739. <https://doi.org/10.1007/s00366-020-01031-w>
- [28] V. Kumar, S. J. Singh, V. H. Saran, and S. P. Harsha, Vibration characteristics of porous FGM plate with variable thickness resting on Pasternak's foundation, *Eur. J. Mech. A/Solids*, 85 (2021) 104124. <https://doi.org/10.1016/j.euromechsol.2020.104124>
- [29] L. Hadji and M. Avcar, Free Vibration Analysis of FG Porous Sandwich Plates under Various Boundary Conditions, *J. Appl. Comput. Mech.*, 7 (2021) 505–519. <https://doi.org/10.22055/jacm.2020.35328.2628>
- [30] S. Oveissi, S. A. Eftekhari, and D. Toghraie, Longitudinal vibration and instabilities of carbon nanotubes conveying fluid considering size effects of nanoflow and nanostructure, *Physica E Low Dimens. Syst. Nanostruct.*, 83 (2016) 164–173. <https://doi.org/10.1016/j.physe.2016.05.010>
- [31] S. Oveissi, D. Toghraie, and S. A. Eftekhari, Longitudinal vibration and stability analysis of carbon nanotubes conveying viscous fluid, *Physica E Low Dimens. Syst. Nanostruct.*, 83 (2016) 275–283. <https://doi.org/10.1016/j.physe.2016.05.004>
- [32] H. M. S. and Y. K. Mohammadi, A simplified isogeometric approach for vibrational analysis of nanocomposite panels with a free-form curve, *Thin-Walled Struct.*, 183 (2023) 110426. <https://doi.org/10.1016/j.physe.2016.05.010>
- [33] H. Mohammadi, Isogeometric approach for thermal buckling analysis of FG graphene platelet reinforced composite trapezoidally corrugated laminated panels, *Eng. Anal. Bound. Elem.*, 151 (2023) 244–254. <https://doi.org/10.1016/j.enganabound.2023.03.007>
- [34] P. Wang, P. Yuan, S. Sahmani, and B. Safaei, Size-dependent nonlinear harmonically soft excited oscillations of nonlocal strain gradient FGM composite truncated conical microshells with magnetostrictive facesheets, *Mech. Based Des. Struct. Mach.*, 51 (2023) 1–27. <https://doi.org/10.1080/15397734.2021.1903495>
- [35] N. D. Dat, N. van Thanh, V. MinhAnh, and N. D. Duc, Vibration and nonlinear dynamic analysis of sandwich FG-CNTRC plate with porous core layer, *Mech. Adv. Mater. Struct.*, 29 (2022) 1431–1448. <https://doi.org/10.1080/15376494.2020.1822476>
- [36] A. Mouthanna, S. H. Bakhy, and M. Al-Waily, Analytical Investigation of Nonlinear Free Vibration of Porous Eccentrically Stiffened Functionally Graded Sandwich Cylindrical Shell Panels, *Iran. J. Sci. Technol. Trans. Mech. Eng.*, (2022). <https://doi.org/10.1007/s40997-022-00555-4>
- [37] A. Mouthanna, S. H. Bakhy, and M. Al-Waily, Frequency Of Non-Linear Dynamic Response Of A Porous Functionally Graded Cylindrical Panels, *J. Teknol.*, 84 (2022) 59–68. <https://doi.org/10.11113/jurnalteknologi.v84.18422>
- [38] S. S. Mirjavadi, M. Forsat, M. R. Barati, and A. M. S. Hamouda, Geometrically nonlinear vibration analysis of eccentrically stiffened porous functionally graded annular spherical shell segments, *Mech. Based Des. Struct. Mach.*, 50 (2022) 2206–2220. <https://doi.org/10.1080/15397734.2020.1771729>

- [39] A. Karakoti, S. Pandey, and V. R. Kar, Nonlinear transient analysis of porous P-FGM and S-FGM sandwich plates and shell panels under blast loading and thermal environment, *Thin-Walled Struct.*, 173 (2022) 108985. <https://doi.org/10.1016/j.tws.2022.108985>
- [40] E. , M. A. R. , C. Ö. , & A.-P. A. R. Sobhani, Free-damped vibration tangential wave responses of FG-sandwich merged hemispherical-cylindrical shells under effects of artificial springs at merging and boundary conditions, *Eng .Struct.*, 284 (2023) 115958. <https://doi.org/10.1016/j.engstruct.2023.115958>
- [41] H. Mohammadi, Isogeometric free vibration analysis of trapezoidally corrugated FG-GRC laminated panels using higher-order shear deformation theory, *Structures*, 48 (2023) 642–656. <https://doi.org/10.1016/j.tws.2022.108985>
- [42] H. Mohammadi, On the mechanical buckling analysis of FG-GRC laminated plates with temperature-dependent material properties using isogeometric approach, *Int. J. Struct. Stab. Dyn.*, 23 (2023) 2350092. <https://doi.org/10.1142/S021945542350092X>
- [43] H. , O. W. and M. S. Mohammadi, Isogeometric technique for dynamic instability analysis of nanocomposite folded plates based on higher-order shear deformation theory, *Thin-Walled Struct.*, 177 (2022) 109467. <https://doi.org/10.1016/j.tws.2022.109467>
- [44] H. Ahmadi, A. Bayat, and N. D. Duc, Nonlinear forced vibrations analysis of imperfect stiffened FG doubly curved shallow shell in thermal environment using multiple scales method, *Compos. Struct.*, 256 (2021) 113090. <https://doi.org/10.1016/j.compstruct.2020.113090>
- [45] P. van Vinh, “Nonlocal free vibration characteristics of power-law and sigmoid functionally graded nanoplates considering variable nonlocal parameter, *Physica E Low Dimens. Syst. Nanostruct.*, 135 (2022) 114951. <https://doi.org/10.1016/j.physe.2021.114951>
- [46] Y. Liu, Z. Qin, and F. Chu, Nonlinear forced vibrations of functionally graded piezoelectric cylindrical shells under electric-thermo-mechanical loads, *Int. J. Mech. Sci.*, 201 (2021) 106474. <https://doi.org/10.1016/j.ijmecsci.2021.106474>
- [47] D. G. Ninh and D. H. Bich, Nonlinear thermal vibration of eccentrically stiffened Ceramic-FGM-Metal layer toroidal shell segments surrounded by elastic foundation, *Thin-Walled Struct.*, 104 (2016) 198–210. <https://doi.org/10.1016/j.tws.2016.03.018>
- [48] T. Fu, X. Wu, Z. Xiao, and Z. Chen, Thermoacoustic response of porous FGM cylindrical shell surround by elastic foundation subjected to nonlinear thermal loading, *Thin-Walled Struct.*, 156 (2020) 106996. <https://doi.org/10.1016/j.tws.2020.106996>
- [49] S. S. Mirjavadi, M. Forsat, M. R. Barati, and A. M. S. Hamouda, Geometrically nonlinear vibration analysis of eccentrically stiffened porous functionally graded annular spherical shell segments, *Mech. Based Des. Struct. Mach.*, 50 (2022) 2206–2220. <https://doi.org/10.1080/15397734.2020.1771729>
- [50] N. Dinh Duc, P. Dinh Nguyen, and N. Dinh Khoa, Nonlinear dynamic analysis and vibration of eccentrically stiffened S-FGM elliptical cylindrical shells surrounded on elastic foundations in thermal environments, *Thin-Walled Struct.*, 117 (2017) 178–189. <https://doi.org/10.1016/j.tws.2017.04.013>
- [51] M. Darabi, M. Darvizeh, and A. Darvizeh, Non-linear analysis of dynamic stability for functionally graded cylindrical shells under periodic axial loading, *Compos. Struct.*, 83 (2008) 201–211. <https://doi.org/10.1016/j.compstruct.2007.04.014>
- [52] A. Aliyari Parand and A. Alibeigloo, Static and vibration analysis of sandwich cylindrical shell with functionally graded core and viscoelastic interface using DQM, *Compos. B Eng.*, 126 (2017) 1–16. <https://doi.org/10.1016/j.compositesb.2017.05.071>
- [53] T. I. Thinh, D. H. Bich, T. M. Tu, and N. Van Long, Nonlinear analysis of buckling and postbuckling of functionally graded variable thickness toroidal shell segments based on improved Donnell shell theory, *Compos. Struct.*, 243 (2020) 112173. <https://doi.org/10.1016/j.compstruct.2020.112173>
- [54] N. D. Duc, Nonlinear dynamic response of imperfect eccentrically stiffened FGM double curved shallow shells on elastic foundation, *Compos. Struct.*, 99 (2013) 88–96. <https://doi.org/10.1016/j.compstruct.2012.11.017>
- [55] F. Alijani, M. Amabili, K. Karagiozis, and F. Bakhtiari-Nejad, Nonlinear vibrations of functionally graded doubly curved shallow shells, *J. Sound Vib.*, 330 (2011) 1432–1454. <https://doi.org/10.1016/j.jsv.2010.10.003>
- [56] H. Matsunaga, Free vibration and stability of functionally graded shallow shells according to a 2D higher-order deformation theory, *Compos Struct.*, 84 (2008) 132–146. <https://doi.org/10.1016/j.compstruct.2007.07.006>
- [57] Y. Liu, Y. Hu, T. Liu, J. L. Ding, and W. H. Zhong, Mechanical behavior of high density polyethylene and its carbon nanocomposites under quasi-static and dynamic compressive and tensile loadings, *Polym .Test.*, 41 (2015) 106–116. <https://doi.org/10.1016/j.polymertesting.2014.11.003>
- [58] N. Bonnheim, F. Ansari, M. Regis, P. Bracco, and L. Pruitt, Effect of carbon fiber type on monotonic and fatigue properties of orthopedic grade PEEK, *J. Mech. Behav. Biomed. Mater.*, 90 (2019) 484–492. <https://doi.org/10.1016/j.jmbbm.2018.10.033>